The Canadian Journal of Mineralogy and Petrology
ISSN 2817-1713
Vol. 61, pp. 203-213 (2023)
DOI: 10.3749/2200049

RAYDEMARKITE, THE NATURAL ANALOGUE OF SYNTHETIC α-$MoO_3 \cdot H_2O$, FROM COOKES PEAK, LUNA COUNTY, NEW MEXICO, USA

HEXIONG YANG[§]

Department of Geosciences, University of Arizona, 1040 E. 4th Street, Tucson, Arizona 85721-0077, USA

XIANGPING GU

School of Geosciences and Info-Physics, Central South University, Changsha, Hunan 410083, China

FRANCIS X. SOUSA, RONALD B. GIBBS, JAMES A. MCGLASSON, AND ROBERT T. DOWNS

Department of Geosciences, University of Arizona, 1040 E. 4th Street, Tucson, Arizona 85721-0077, USA

ABSTRACT

A new mineral species, raydemarkite, ideally $MoO_3 \cdot H_2O$, was discovered in an unnamed short adit on the Summit group of claims near Cookes Peak, Luna County, New Mexico, USA. It occurs as sprays of acicular or prismatic crystals on a matrix consisting mainly of quartz and pyrite. Individual crystals of raydemarkite are up to 1.00 × 0.10 × 0.06 mm. Associated minerals include sidwillite, ilsemannite, jordisite, powellite, anhydrite, gypsum, bouškaite, pyrite, and quartz. Raydemarkite is colorless in transmitted light and transparent with white streak and vitreous luster. It is flexible and has a Mohs hardness of ~1½; cleavage is perfect on {100} and {001}. Twinning is common on (010). The measured and calculated densities are 3.44(5) and 3.41 g/cm^3, respectively. Raydemarkite is insoluble in water or hydrochloric acid. An electron microprobe analysis yielded an empirical formula, based on 4 O *apfu*, of $MoO_3 \cdot H_2O$.

Raydemarkite is the natural analogue of the α-form of $MoO_3 \cdot H_2O$, which was first synthesized over a century ago (Rosenheim & Davidsohn 1903). Its crystal structure was solved using single-crystal X-ray diffraction data. It is triclinic, crystallizing in space group $P\bar{1}$ and the unit-cell parameters $a = 7.3750(2)$, $b = 3.70920(10)$, $c = 6.6833(2)$ Å, $\alpha = 108.1080(10)$, $\beta = 112.779(2)$, $\gamma = 91.7420(10)°$, $V = 157.828(8)$ Å^3, and $Z = 2$. The crystal structure of raydemarkite is built up from isolated double chains of highly distorted, edge-sharing $MoO_5(H_2O)$ octahedra parallel to [010] that are linked together through hydrogen bonds, accounting for its acicular/prismatic morphology and the marked flexibility. Synthetic hemihydrate $MoO_3 \cdot 1/2H_2O$ (monoclinic, space group $P2_1/m$) can be regarded as a combination of molybdite and raydemarkite both structurally and chemically.

Keywords: raydemarkite, molybdenum trioxide hydrates, molybdic acids, crystal structure, X-ray diffraction, Cookes Peak.

INTRODUCTION

Molybdenum trioxide (MoO_3) and its related hydrates, namely molybdic acids, ($MoO_3 \cdot nH_2O$, n = 2, 1, 1/2, and 1/3) have been a research subject for over a century owing to their versatile applications in electronics, catalysis, sensors, energy-storage units, field emission devices, lubricants, super-conductors, thermal materials, biosystems, chromogenics, and electrochromic systems (*cf*. de Castro *et al*. 2017). Thus far, five polymorphs of MoO_3 have been identified, including the orthorhombic α-form (Bräkken 1931, Wooster 1931, Andersson & Magléni 1950, Kihlborg 1963, Sitepu 2009), which has been found in nature and named molybdite (Čech & Povondra 1963). In addition, four other metastable polymorphs are known: monoclinic β-MoO_3 and β′-MoO_3 modifications with the 3D ReO_3 structure

§ *Corresponding author e-mail address*: hyang@arizona.edu

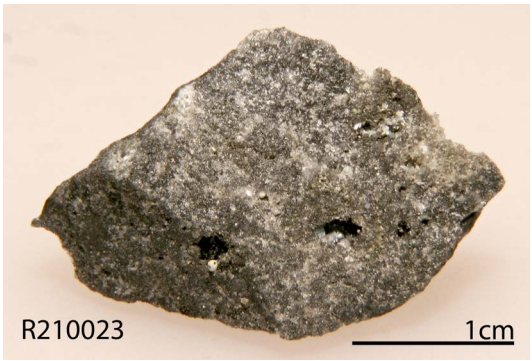

FIG. 1. A specimen on which the new mineral raydemarkite was found.

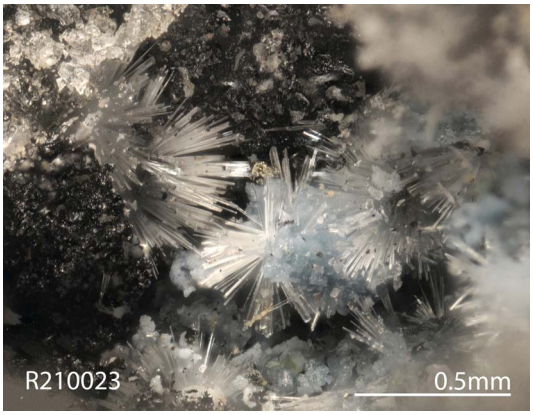

FIG. 2. A microscopic view of sprays of white acicular or prismatic crystals of raydemarkite.

(McCarron 1986, Parise *et al*. 1991, Mougin *et al*. 2000, Liu *et al*. 2009), the high-pressure monoclinic ($P2_1/m$) MoO_3-II phase (McCarron & Calabrese 1991), and the hexagonal ($P6_3/m$ or $P6_3$) h-MoO_3 phase (Guo *et al*. 1994). Among the molybdenum trioxide hydrates, six different phases have been reported: (1) monoclinic $P2_1/n$ dihydrate $MoO_3{\cdot}2H_2O$ (Krebs 1972, Cesbron & Ginderow 1985), (2) monoclinic $P2/m$ yellow dihydrate $MoO_3{\cdot}2H_2O$ (Schultén 1903, Lindqvist 1950), (3) triclinic $P\bar{1}$ white monohydrate α-$MoO_3{\cdot}H_2O$ (Rosenheim & Davidsohn 1903, Böschen & Krebs 1974, Oswald *et al*. 1975), (4) monoclinic $P2_1/c$ yellow monohydrate β-$MoO_3{\cdot}H_2O$ (Rosenheim & Davidsohn 1903, Günter 1972, Boudjada *et al*. 1993), (5) monoclinic $P2_1/m$ hemihydrate $MoO_3{\cdot}1/2H_2O$ (Fellows *et al*. 1983, Bénard *et al*. 1994), and (6) hexagonal $P6_3/m$ $MoO_3{\cdot}1/3H_2O$ (Fu *et al*. 2005, Deki *et al*. 2009, Zhao *et al*. 2009, Lunk *et al*. 2010). Of these six $MoO_3{\cdot}nH_2O$ phases, only the dihydrate, sidwillite ($MoO_3{\cdot}2H_2O$, $P2_1/n$; Cesbron & Ginderow 1985), has been found in nature[1].

This study reports on the discovery of the new mineral species, raydemarkite, which is the natural analogue of the α-form of monohydrate $MoO_3{\cdot}H_2O$. The new mineral is named in honor of Mr. Ramon (Ray) S. Demark (b. 1937), a long-time New Mexico mineral collector. After receiving his B.S. in geology from the University of Illinois, Ray served in the U.S. Navy as an aviation officer for 20 years and then continued to teach for 11 more years through the Navy Junior Reserve Officer Training Corp. He began collecting minerals at about age 10 while growing up in Illinois. Ray has been a mineral enthusiast, mineral dealer, and co-owner of mining claims producing mineral specimens for museums and collectors. He has mentored and encouraged young and old mineral collectors throughout his many years in the hobby. Ray is an active member of the Albuquerque Gem and Mineral Club and has authored and co-authored numerous articles for *Mineralogical Record*, *Rocks and Minerals*, and *Mineral News*. He is a co-founder of the New Mexico Mineral Symposium held annually at the New Mexico Institute of Mining and Technology in Socorro, New Mexico, and has presented at every symposium since 1980. Ray has contributed many specimens to mineral museums over the years and is a strong supporter of the New Mexico Bureau of Geology Mineral Museum in Socorro, New Mexico. The new mineral and its name have been approved by the Commission on New Minerals, Nomenclature and Classification (CNMNC) of the IMA (IMA 2022-015). Parts of the cotype samples have been deposited at the Alfie Norville Gem and Mineral Museum (Catalog # 22717) and the RRUFF Project (deposition #R210023) at the University of Arizona.

SAMPLE DESCRIPTION AND EXPERIMENTAL METHODS

Occurrence, physical and chemical properties, and Raman spectra

Raydemarkite was found on specimens (Fig. 1) collected by Mr. Ray Demark on February 19, 2016, in an unnamed short adit on the Summit group of claims (32° 33′ 47″ N and 107° 43′ 48″ W) near Cookes Peak, at the southern end of the Cookes Range, Luna County, New Mexico, USA. It occurs as sprays of acicular or prismatic crystals that are elongated along [010] (Figs. 2 and 3) on a matrix of mainly quartz and pyrite (Fig. 1). Individual crystals of raydemarkite are

[1] Subsequent to acceptance of this article, hemihydrate $MoO_3{\cdot}1/2H_2O$ was discovered in nature; this mineral has been named zhenruite (IMA2022-050).

FIG. 3. A microscopic view of radiating sprays of colorless prismatic crystals of raydemarkite associated with yellow-green sidwillite crystals (photo by Andreas Schloth).

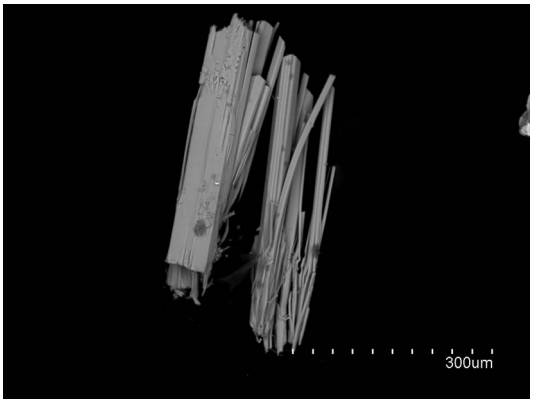

FIG. 4. A backscattered electron image of prismatic raydemarkite crystals showing perfect cleavages and good flexibility.

up to 1.00 × 0.10 × 0.06 mm. Associated minerals include sidwillite, ilsemannite, jordisite, powellite, fluorite, anhydrite, gypsum, bouškaite, pyrite, and quartz.

The Summit group and its claims represent one of the largest lead, zinc, and silver producers in Luna County (McLemore *et al*. 2001). They include a number of adits, shafts, pits, and trenches, many of which are rich in fluorite and are considered to be products resulting from the interaction of hydrothermal solutions derived from a nearby granodiorite with limestone units located beneath impermeable shales which were accompanied by silicification leading to formation of jasperoids. The upper levels of the mines were highly oxidized and have been completely mined out. A more detailed geology and mineralogy of Cookes Peak mining district has been presented by Simmons (2019).

Raydemarkite is colorless in transmitted light and transparent with white streak and vitreous luster. It is flexible with a Mohs hardness of ~1½; cleavage is perfect on {100} and {001} (Fig. 4). No twinning was observed visually, but it was detected with X-ray diffraction as a 180° rotation about the *b* axis. The measured (by flotation in heavy liquids) and calculated densities are 3.44(5) and 3.41 g/cm^3, respectively. No optical data were measured because the indices of refraction were determined to be too high for measurement with available index liquids. The calculated average index of refraction is 1.85 for the empirical formula based on the Gladstone-Dale relationship (Mandarino 1981). Raydemarkite is insoluble in water and hydrochloric acid.

The chemical composition of raydemarkite was determined with a Cameca SX-100 electron microprobe operated at 15 keV and 20 nA with a beam size of 1 μm. The standards used include powellite for Mo and stibnite for Sb. The average of ten analysis points gives (wt.%) MoO_3 = 88.48(99), Sb_2O_3 = 0.13(14), with the total = 88.62(88). The empirical formula, calculated on the basis of 4 O *apfu* and assuming one H_2O group (based on results from the crystal-structure refinement), is $(Mo_{1.00})O_3 \cdot H_2O$.

The Raman spectrum (Fig. 5) of raydemarkite was collected from a randomly oriented crystal on a Thermo Almega microRaman system using a solid-state laser with a wavelength of 532 nm and a thermoelectric cooled CCD detector. The laser is partially polarized with 4 cm^{-1} resolution and a spot size of 1 μm. For comparison, the Raman spectra of molybdite, MoO_3, and sidwillite, $MoO_3 \cdot 2H_2O$, from the RRUFF Project (2022a, b) are also plotted in Figure 5.

X-ray crystallography

Both powder and single-crystal X-ray diffraction data for raydemarkite were collected on a Bruker X8 APEX2 CCD X-ray diffractometer equipped with graphite-monochromatized Mo*K*α radiation. The unit-cell parameters refined from the powder X-ray diffraction data (Table 1) with the program by Downs *et al*. (1993) are a = 7.385(5), b = 3.704(3), c = 6.689(5) Å, α = 108.21(7), β =112.81(6), γ = 91.69(6)°, and V = 157.80(14) Å^3.

All raydemarkite crystals examined were found to be pervasively twinned on (010). The X-ray diffraction data used for the structure analysis were collected from a prismatic crystal (0.06 × 0.03 × 0.03 mm) with frame widths of 0.5° in ω and 30 s counting time per frame and processed using the Bruker TWINABS software, yielding a twin ratio of 86:14. The systematic absences of reflections suggest possible

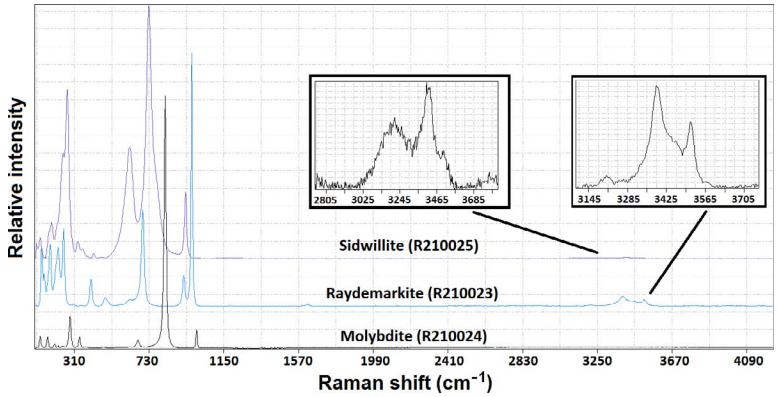

FIG. 5. Raman spectra of raydemarkite, molybdite, and sidwillite

space group $P\bar{1}$ or $P1$. The crystal structure was solved and refined in $P\bar{1}$ using SHELX2018 (Sheldrick 2015a, b); $P\bar{1}$ was chosen as it produced better refinement statistics in terms of bond lengths and angles, atomic displacement parameters, and R factors. The refinement statistics are given in Table 2. All H atoms were located through the difference Fourier syntheses. Final atomic coordinates and displacement parameters for raydemarkite are given in Tables 3 and 4, respectively. Selected bond distances and the H-bonding scheme are presented in Tables 5 and 6, respectively[2].

DISCUSSION

Crystal structure

Raydemarkite is the natural analogue of the so-called white α-$MoO_3 \cdot H_2O$ phase. It, along with the yellow β-$MoO_3 \cdot H_2O$ phase, was first synthesized over a century ago (Rosenheim & Davidsohn 1903). The crystal structure of synthetic raydemarkite was determined by Böschen & Krebs (1974) and Oswald *et al.* (1975). In this study, the unit-cell setting used by Oswald *et al.* (1975) was adopted. The structure of raydemarkite is built from isolated double chains of $MoO_5(H_2O)$ octahedra parallel to [010] (Fig. 6). Each octahedron shares two common edges with neighboring ones. The double octahedral chains in molybdite, MoO_3 (Kihlborg 1963, Sitepu 2009) are topologically identical to those in raydemarkite (Fig. 7), but instead are directly linked to one another by sharing octahedral corners to form layers parallel to (010) (Fig. 8). In contrast, the octahedral double chains in raydemarkite, which account for the acicular morphology, are linked together only through hydrogen bonds, which account for the marked flexibility. Accordingly, the MoO_6 layers in molybdite can be considered a condensation product of the raydemarkite chains (Böschen & Krebs 1974).

The $MoO_5(H_2O)$ octahedron in raydemarkite is considerably distorted, with two short Mo–O bonds of 1.693 and 1.694 Å to the terminal O1 and O3 atoms, respectively, two intermediate Mo–O bonds of 1.958 Å to the bridging O2 atoms, and two long Mo–O bond distances of 2.267 and 2.329 Å to the third bridging O2 atom and the H_2O (O4) molecule, respectively (Table 5). The octahedral distortion indices, as defined by angle variance and quadratic elongation (Robinson *et al.* 1971), are 159.6 and 1.064, respectively. Similar highly distorted octahedra have also been observed in other Mo-bearing materials, such as molybdite, MoO_3 (Kihlborg 1963, Sitepu 2009); sidwillite, $MoO_3 \cdot 2H_2O$ (Krebs 1972, Cesbron & Ginderow 1985); and $MoO_3 \cdot 1/2H_2O$ (Bénard *et al.* 1994).

Raman spectra

Band assignments for the Raman spectra of raydemarkite were made based on previous studies on $MoO_3 \cdot 2H_2O$, $MoO_3 \cdot H_2O$ (both α- and β-phases) and $MoO_3 \cdot 1/2H_2O$ (Saleem & Aruldhas 1983, Chandra *et al.* 1987, Seguin *et al.* 1995, Oyerinde *et al.* 2008, Liu *et al.* 2009). The two weak bands at 3394 and 3515 cm^{-1} are assigned to the O–H stretching vibrations, and a very weak band at 1620 cm^{-1} is assigned to the H–O–H bending vibrations in H_2O. The strongest band at 970 cm^{-1} and the weak band at 925 cm^{-1} are attributed to the Mo–O symmetric and antisymmetric stretching vibrations within the MoO_6 group, respectively. The bands between 370 and 700 cm^{-1} are ascribed to the O–Mo–O bending vibrations

[2] A CIF is available as supplementary data, available from the Depository of Unpublished Data on the MAC website (http://mineralogicalassociation.ca/), document "Raydemarkite, CM60, 22-00049".

TABLE 1. POWDER X-RAY DIFFRACTION DATA FOR RAYDEMARKITE

I%	$d_{obs.}$	$d_{calc.}$	h	k	l
18	6.693	6.706	1	0	0
100	5.759	5.772	0	0	1
7	3.632	3.633	$\bar{2}$	0	1
7	3.472	3.466	0	1	0
40	3.334	3.321	$\bar{1}$	1	0
36	3.277	3.269	$\bar{1}$	$\bar{1}$	1
16	3.181	3.177	$\bar{1}$	0	2
18	3.058	3.055	1	$\bar{1}$	1
16	2.892	2.883	1	1	0
7	2.807	2.808	$\bar{1}$	$\bar{1}$	2
7	2.736	2.729	$\bar{1}$	1	1
6	2.482	2.483	2	0	1
5	2.458	2.459	$\bar{3}$	0	1
2	2.352	2.353	2	$\bar{1}$	1
3	2.289	2.290	$\bar{3}$	0	2
10	2.235	2.235	3	0	0
3	2.130	2.131	$\bar{1}$	$\bar{1}$	3
8	2.099	2.096	$\bar{1}$	0	3
5	2.052	2.054	$\bar{2}$	$\bar{1}$	3
5	2.016	2.014	$\bar{2}$	1	2
2	1.968	1.969	$\bar{3}$	$\bar{1}$	1
2	1.924	1.924	0	0	3
2	1.904	1.904	$\bar{3}$	0	3
13	1.852	1.848	0	$\bar{2}$	1
10	1.840	1.841	3	0	1
3	1.829	1.830	3	$\bar{1}$	1
2	1.810	1.805	1	$\bar{2}$	1
5	1.793	1.789	0	$\bar{2}$	2
3	1.766	1.767	1	$\bar{1}$	3
4	1.747	1.747	3	1	0
3	1.715	1.733	0	2	0
2	1.680	1.681	1	1	2
3	1.671	1.670	$\bar{4}$	1	1
5	1.647	1.647	$\bar{2}$	$\bar{1}$	4
5	1.632	1.632	$\bar{4}$	$\bar{1}$	2
4	1.622	1.623	$\bar{4}$	1	0
4	1.608	1.604	$\bar{2}$	1	3
6	1.586	1.586	$\bar{4}$	1	2
4	1.573	1.574	$\bar{4}$	$\bar{1}$	3
4	1.568	1.568	$\bar{4}$	$\bar{1}$	1
3	1.539	1.541	$\bar{3}$	0	4
1	1.527	1.527	2	$\bar{2}$	2
2	1.478	1.478	3	1	1
3	1.473	1.473	4	$\bar{1}$	1
3	1.461	1.460	3	$\bar{2}$	1
3	1.443	1.442	2	2	0
3	1.431	1.431	2	0	3
3	1.417	1.418	$\bar{1}$	$\bar{2}$	4
1	1.392	1.391	$\bar{3}$	$\bar{2}$	1

TABLE 2. CRYSTALLOGRAPHIC DATA FOR RAYDEMARKITE

	Natural raydemarkite	Synthetic raydemarkite
Ideal formula	$MoO_3 \cdot H_2O$	$MoO_3 \cdot H_2O$
Crystal symmetry	Triclinic	Triclinic
Space group	$P\bar{1}$	$P\bar{1}$
a (Å)	7.3750(2)	7.388
b (Å)	3.70920(10)	3.700
c (Å)	6.6833(2)	6.673
α (°)	108.1080(10)	107.8
β (°)	112.779(2)	113.6
γ (°)	91.7420(10)	91.2
V (Å^3)	157.828(8)	156.99
Z	2	2
ρ_{cal} (g/cm^3)	3.408	3.43
2θ range for data collection (°)	$\leq$66.41	$\leq$40.0
No. of reflections collected	8180	747
No. of independent reflections	1184	295
No. of reflections with $I > 2\sigma(I)$	1116	229
No. of parameters refined	55	
R(int)	0.022	0.053
Final R_1, wR_2 factors [$I > 2\sigma(I)$]	0.017, 0.039	0.088
Goodness-of-fit	1.085	
Reference	This study	Oswald *et al.* (1975)

TABLE 3. FRACTIONAL ATOMIC COORDINATES AND EQUIVALENT ISOTROPIC DISPLACEMENT PARAMETERS (Å^2) FOR RAYDEMARKITE

Atom	x	y	z	U_{iso}*/U_{eq}
Mo	0.20562 (2)	0.78601 (3)	0.54105 (2)	0.00961 (6)
O1	0.4561 (2)	0.8796 (4)	0.6990 (3)	0.0223 (3)
O2	0.12787 (19)	0.2909 (3)	0.5582 (2)	0.0130 (3)
O3	0.1807 (2)	0.6367 (4)	0.2637 (3)	0.0208 (3)
O4	0.1884 (3)	0.9900 (5)	0.8987 (3)	0.0219 (3)
H1	0.266 (5)	0.986 (8)	0.990 (5)	0.026 (8)*
H2	0.129 (5)	1.122 (9)	0.932 (6)	0.036 (9)*

within the MoO_6 group. The bands below 290 cm^{-1} are mainly associated with the rotational and translational modes of MoO_6 and H_2O groups and lattice vibrations.

Bond-valence sums, calculated using the parameters given by Brown (2009) (Table 7), indicate that O1 and O3 are noticeably under-bonded. Their deficiencies in the bond valences are compensated by

TABLE 4. ATOMIC DISPLACEMENT PARAMETERS (Å^2) FOR RAYDEMARKITE

Atom	U^{11}	U^{22}	U^{33}	U^{12}	U^{13}	U^{23}
Mo	0.00951 (9)	0.00749 (8)	0.01199 (9)	0.00223 (5)	0.00391 (6)	0.00430 (6)
O1	0.0131 (7)	0.0242 (7)	0.0272 (8)	0.0029 (5)	0.0044 (6)	0.0108 (6)
O2	0.0122 (6)	0.0086 (5)	0.0192 (7)	0.0034 (4)	0.0057 (5)	0.0070 (5)
O3	0.0282 (8)	0.0203 (6)	0.0173 (7)	0.0049 (6)	0.0135 (7)	0.0061 (6)
O4	0.0235 (8)	0.0265 (8)	0.0125 (8)	0.0093 (7)	0.0047 (7)	0.0055 (6)

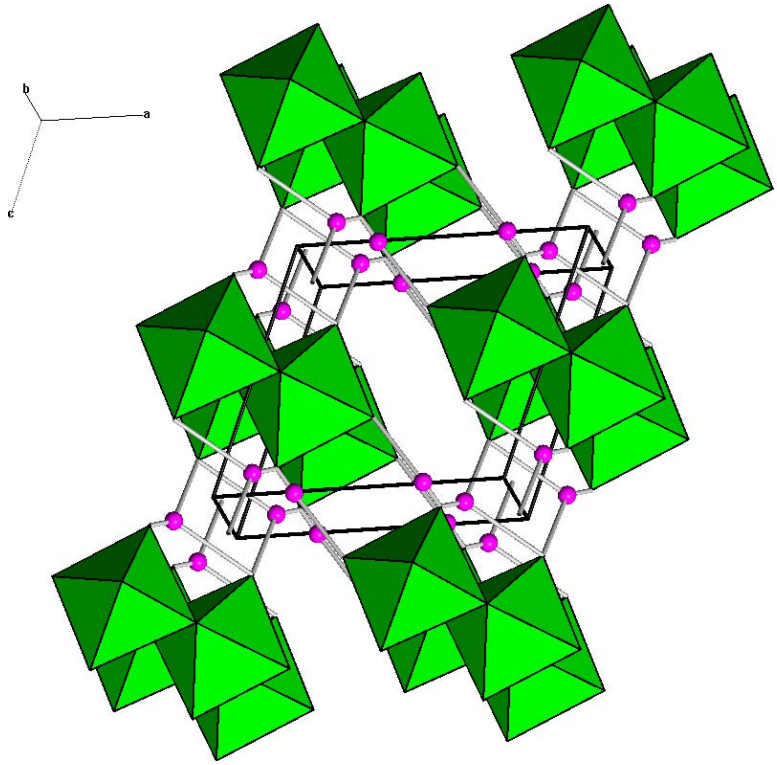

FIG. 6. The crystal structure of raydemarkite, showing isolated double chains of $MoO_5(H_2O)$ octahedra parallel to [010], which are linked together through hydrogen bonds. Green octahedra and pink spheres represent $MoO_5(H_2O)$ groups and H atoms, respectively.

TABLE 5. SELECTED BOND DISTANCES (Å) FOR RAYDEMARKITE

		Natural raydemarkite	Synthetic raydemarkite
Mo	–O1	1.6929(14)	1.66(3)
	–O3	1.6943(14)	1.65(4)
	–O2	1.9577(10)	1.91(3)
	–O2′	1.9585(10)	1.98(3)
	–O2	2.2671(12)	2.28(3)
	–O4	2.3286(15)	2.37(3)
<*M*–O>		1.9832	1.975
Reference		This study	Oswald *et al.* (1975)

hydrogen bonds, as both are engaged in the hydrogen bonding as acceptors (Table 6). According to the correlation between O–H stretching vibrational frequencies and O–H···O hydrogen bond lengths for minerals (Libowitzky 1999), the Raman band at 3394 cm^{-1} corresponds well with the O–O distances (O4–H1-O1 and O4–H2-O3) of 2.83–2.86 Å and that at 3515 cm^{-1} with the O–O distance (O4–H2-O3) of 3.06 Å.

Two polymorphs of monohydrate $MoO_3 \cdot H_2O$ have been reported: the triclinic ($P\bar{1}$) α-form, namely raydemarkite (Böschen & Krebs 1974, Oswald *et al.* 1975, this study) and the yellow monoclinic ($P2_1/c$) β-

TABLE 6. HYDROGEN BONDING GEOMETRY (Å, °) IN RAYDEMARKITE

	D–H (Å)	H-A (Å)	D-A (Å)	<(DHA) (°)
O4–H1-O1	0.75(4)	2.09(4)	2.827(2)	169(3)
O4–H2-O3	0.81(4)	2.21(4)	2.859(2)	138(3)
O4–H2-O3	0.81(4)	2.46(4)	3.064(2)	133(3)

TABLE 7. BOND-VALENCE SUMS FOR RAYDEMARKITE

	Mo	Sum
O1	1.784	1.784
O2	0.872	2.121
	0.870	
	0.378	
O3	1.777	1.777
O4	0.320	0.320
Sum	6.001	

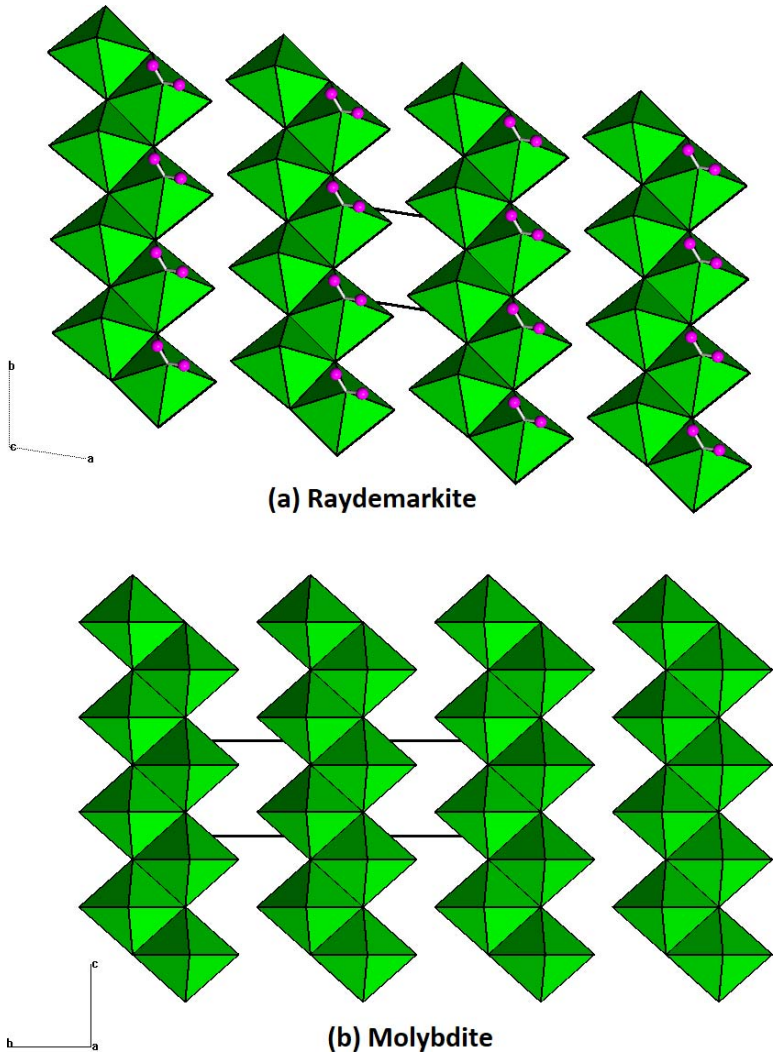

FIG. 7. Comparison of double chains of MoO_6 octahedra in (a) raydemarkite and (b) molybdite (Sitepu 2009) showing their topological resemblance. For raydemarkite, the legend is the same as in Figure 5.

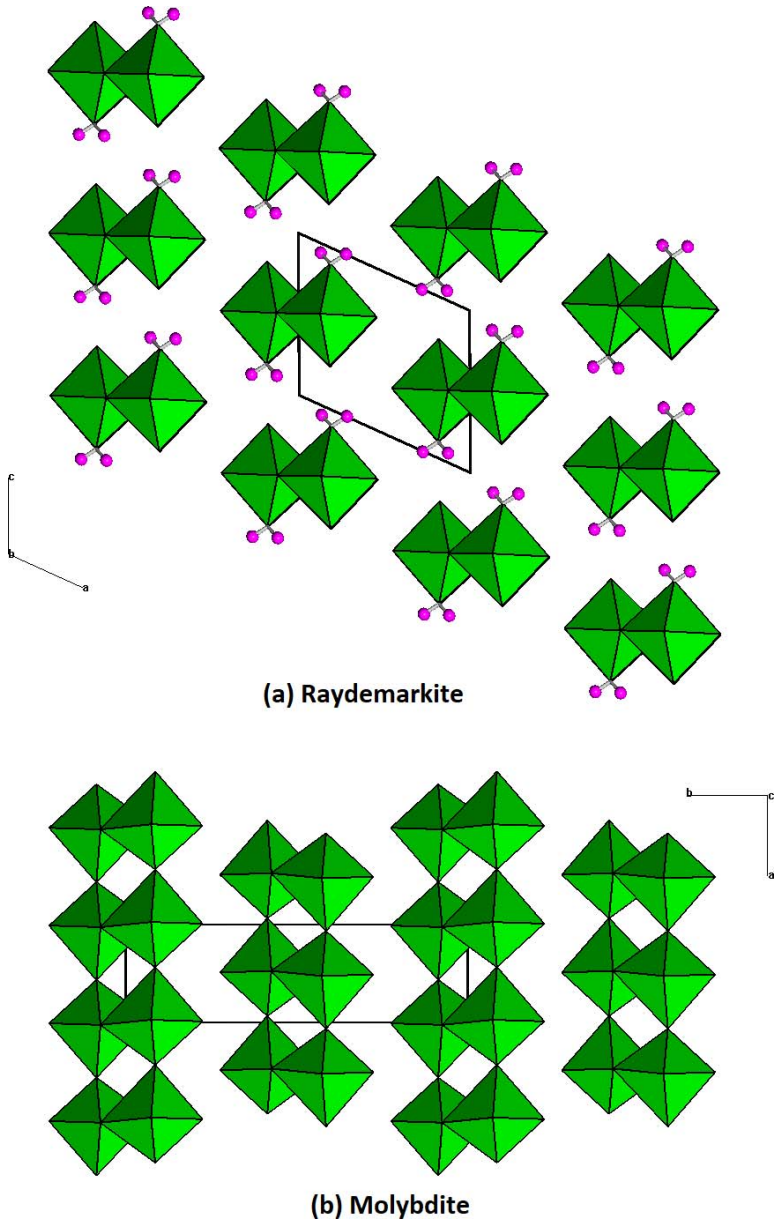

FIG. 8. Comparison of the linkage between the MoO_6 octahedral double chains in (a) raydemarkite and (b) molybdite. The legend for raydemarkite is the same as in Figure 5.

form (Günter 1972, Boudjada *et al*. 1993). The MoO_6 octahedra in the β-form share corners to form layers that are topologically identical to those in sidwillite (Krebs 1972, Cesbron & Ginderow 1985), which differs from the MoO_6 octahedra that share edges in raydemarkite to form layers. Therefore, it is conceivable that, relative to raydemarkite, the β-form of $MoO_3{\cdot}H_2O$ will be energetically favored to form through the dehydration of sidwillite. In fact, Günter (1972) and Boudjada *et al*. (1993) have demonstrated that sidwillite dehydrates to form the β-phase of $MoO_3{\cdot}H_2O$ between 60 and 80 °C through a topotactic mechanism. Thus far, there is no report of the formation of raydemarkite through the dehydration

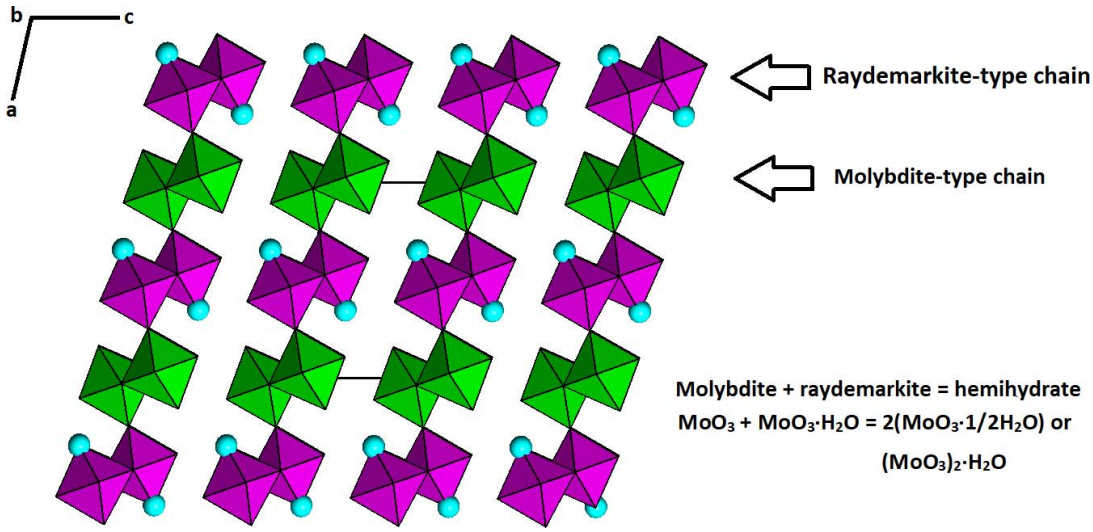

FIG. 9. Crystal structure of hemihydrate $MoO_3 \cdot 1/2H_2O$ (Bénard *et al*. (1994). The aqua spheres and green and purple octahedra represent H_2O, MoO_6, and $MoO_5(H_2O)$ groups, respectively.

of sidwillite. Nevertheless, both α- and β-forms of $MoO_3 \cdot H_2O$ will dehydrate upon heating between 110 and 160 °C to become molybdite, MoO_3 (Günter 1972, Oswald *et al*. 1975, Boudjada *et al*. 1993).

Bénard *et al*. (1994) determined the crystal structure of hemihydrate $MoO_3 \cdot 1/2H_2O$ using powder X-ray diffraction data and showed that it consists of isolated layers formed by two types of double octahedral chains extending along [010] (Fig. 9): (1) type-A chains, built up from strongly distorted $[MoO_6]$ octahedra and (2) type-B chains, composed of $[MoO_5(H_2O)]$ octahedra. These two types of chains alternate along [100] and are joined together by sharing corners to form octahedral layers parallel to (001). An examination of the hemihydrate $MoO_3 \cdot 1/2H_2O$ structure reveals that its type-A chains have the same configuration as those in molybdite, whereas its type-B chains resemble to those in raydemarkite. In other words, hemihydrate $MoO_3 \cdot 1/2H_2O$ can be regarded as a combination, both structurally and chemically, of molybdite and raydemarkite, as illustrated in Figure 9.

ACKNOWLEDGMENTS

This study was supported by the Feinglos family. We are grateful to Dr. James Evans for handling the review process and Dr. Pietro Vignola for the constructive comments.

REFERENCES

ANDERSSON, G. & MAGNÉLI, A. (1950) On the crystal structure of molybdenum trioxide. *Acta Chemica Scandinavica* **4**, 793–797.

BÉNARD, P., SEQUIN, L., LOUËR, D., & FIGLARZ, M. (1994) Structure of $MoO_3 \cdot 1/2H_2O$ by conventional X-ray powder diffraction. *Journal of Solid State Chemistry* **108**, 170–176.

BÖSCHEN, V.I. & KREBS, B. (1974) Kristallstruktur der 'weissen molybdänsäure' α-$MoO_3.H_2O$. *Acta Crystallographica* **B30**, 1795–1800.

BOUDJADA, N., RODRIGUEZ-CARVAJAL, J., ANNE, M., & FIGLARZ, M. (1993) Dehydration of $MoO_3.2H_2O$: A neutron thermodiffractometry study. *Journal of Solid State Chemistry* **105**, 211–222.

BRÄKKEN, H. (1931) Die kristallstrukturen der trioxyde von chrom, molybdän und wolfram. *Zeitschrift für Kristallographie* **78**, 484–488.

BROWN, I.D. (2009) Recent developments in the methods and applications of the bond valence model. *Chemical Reviews* **109**, 6858–6919.

ČECH, F. & POVONDRA, P. (1963) Natural occurrence of molybdenum trioxide, MoO_3, in Krupka (Molybdite, a new mineral). *Acta Universitatis Carolinae - Geologica* **1**, 1–14.

CESBRON, F. & GINDEROW, D. (1985) La sidwillite, $MoO_3 \cdot 2H_2O$; une nouvelle espèce minérale de Lake

Como, Colorado, U.S.A. *Bulletin de Minéralogie* **108**, 813–823.

Chandra, S., Singh, N., Singh, B., Verma, A.L., Khatri, S.S., & Chakrabarty, T. (1987) Laser Raman spectral studies under D.C. bias on fast proton transport in molybdic acid ($MoO_3 \cdot 2H_2O$). *Journal of Physical and Chemical Solids* **48**, 1165–1171.

de Castro, I.A., Datta, R.S., Ou, J.Z., Castellanos-Gomez, A., Sriram, S., Daeneke, T., & Kalantar-zadeh, K. (2017) Molybdenum oxides – from fundamentals to functionality. *Advanced Materials* **28**, 1701619.

Deki, S., Béléké, A.B., Kotani, Y., & Mizuhata, M. (2009) Liquid phase deposition synthesis of hexagonal molybdenum trioxide thin films. *Journal of Solid State Chemistry* **182**, 2362–2367.

Downs, R.T., Bartelmehs, K.L., Gibbs, G.V., & Boisen, M.B., Jr (1993) Interactive software for calculating and displaying X-ray or neutron powder diffractometer patterns of crystalline materials. *American Mineralogist* **78**, 1104–1107.

Fellows, R.L., Lloyd, M.H., Knight, J.F., & Yakel, H.L. (1983) X-ray diffraction and thermal analysis of molybdenum(VI) oxide hemihydrate: Monoclinic $MoO_3 \cdot 1/2H_2O$. *Inorganic Chemistry* **22**, 2468–2470.

Fu, G., Xu, X., Lu, X., & Wan, H. (2005) Mechanisms of methane activation and transformation on molybdenum oxide based catalysts. *Journal of the American Chemical Society* **127**, 3989–3996.

Günter, J.R. (1972) Topotactic dehydration of molybdenum trioxide-hydrates. *Journal of Solid State Chemistry* **5**, 354–359.

Guo, J., Zavalij, P., & Whittingham, M.S. (1994) Preparation and characterization of a MoO_3 with hexagonal structure. *European Journal of Solid State and Inorganic Chemistry* **31**, 833–842.

Kihlborg, L. (1963) Least squares refinement of the crystal structure of molybdenum trioxide. *Arkiv för Kemi* **21**, 357–364.

Krebs, B. (1972) Die kristallstruktur von $MoO_3 \cdot 2H_2O$. *Acta Crystallographica* **B28**, 2222–2231.

Libowitzky, E. (1999) Correlation of O–H stretching frequencies and O–H···O hydrogen bond lengths in minerals. *Monatshefte für Chemie* **130**, 1047–1059.

Lindqvist, I. (1950) The crystal structure of the yellow molybdic acid, $MoO_3 \cdot 2H_2O$. *Acta Chemica Scandinavica* **4**, 650–657.

Liu, D., Lei, W.W., Hao, J., Liu, D.D., Liu, B.B., Wang, X., Chen, X.H., Cui, Q.L., Zou, G.T., Liu, J., & Jiang, S. (2009) High-pressure Raman scattering and X-ray diffraction of phase transitions in MoO_3. *Journal of Applied Physics* **105**, 023513.

Lunk, H.J., Hartl, H., Hartl, M.A., Fait, M.J., Shenderovich, I.G., Feist, M., Frisk, T.A., Daemen, L.L., Mauder, D., Eckelt, R., & Gurinov, A.A. (2010) "Hexagonal molybdenum trioxide" – known for 100 years and still a fount of new discoveries. *Inorganic Chemistry* **49**, 9400–9408.

Mandarino, J.A. (1981) The Gladstone–Dale relationship. IV. The compatibility concept and its application. *The Canadian Mineralogist* **19**, 441–450.

McCarron, E.M. (1986) β-MoO_3: A metastable analogue of WO_3. *Journal of the Chemical Society, Chemical Communications* **1986**, 336.

McCarron, E.M. & Calabrese, J.C. (1991) The growth and single crystal structure of a high pressure phase of molybdenum trioxide: MoO_3-II. *Journal of Solid State Chemistry* **91**, 121–125.

McLemore, V.T., Donahue, K., Breese, M., Jackson, M.L., Arbuckle, J., & Jones, G. (2001) *Mineral resource assessment of Luna County, New Mexico*. New Mexico Bureau of Geology and Mineral Resources Open-file Report OF-459. New Mexico Bureau of Geology and Mineral Resources, Socorro, New Mexico, United States of America.

Mougin, O., Dubois, J., & Mathieu, F. (2000) Metastable hexagonal vanadium molybdate study. *Journal of Solid State Chemistry* **152**, 353–360.

Oswald, H.R., Gunter, J.R., & Dubler, E. (1975) Topotactic decomposition and crystal structure of white molybdenum trioxide-monohydrate: Prediction of structure by topotaxy. *Journal of Solid State Chemistry* **13**, 330–338.

Oyerinde, O.F., Weeks, C.L., Anbar, A.D., & Spiro, T.G. (2008) Solution structure of molybdic acid from Raman spectroscopy and DFT analysis. *Inorganica Chimica Acta* **361**, 1000–1007.

Parise, J.B., McCarron, E.M., Dreele, R.V., & Goldstone, J.A. (1991) β-MoO_3 produced from a novel freeze drying route. *Journal of Solid State Chemistry* **93**, 193–201.

Robinson, K., Gibbs, G.V., & Ribbe, P.H. (1971) Quadratic elongation: A quantitative measure of distortion in coordination polyhedra. *Science* **172**, 567–570.

Rosenheim, A. & Davidsohn, I. (1903) Die hydrate der molybdänsäure. *Zeitschrift für Anorganische und Allgemeine Chemie* **37**, 314–325.

RRUFF Project (2022a) Molybdite. Available from <http://rruff.info/R210024> [Date accessed: 2021].

RRUFF Project (2022b) Sidwillite. Available from <http://rruff.info/R210025> [Date accessed: 2021].

Saleem, S.S. & Aruldhas, G. (1983) Vibrational spectra of α-molybdic acid-$MoO_3 \cdot H_2O$. *Pramana* **21**, 283–291.

Schultén, A.B.A. (1903) Recherches sur l'arséniate dicalcique. Reproduction artificielle de la pharmacolite et de la haidingerite. *Bulletin de Minéralogie* **26**, 18–24.

Seguin, L., Figlarz, M., Cavagnat, R., & Lasskgues, J.-C. (1995) Infrared and Raman spectra of MoO_3, molybdenum trioxides and $MoO_3 \cdot xH_2O$ molybdenum trioxide hydrates. *Spectrochimica Acta, Part A* **51**, 1323–1344.

Sheldrick, G.M. (2015a) SHELXT – Integrated space-group and crystal structure determination. *Acta Crystallographica* **A71**, 3–8.

Sheldrick, G.M. (2015b) Crystal structure refinement with SHELX. *Acta Crystallographica* **C71**, 3–8.

Simmons, P. (2019) Cookes Peak Mining District, Luna County, New Mexico. *Rocks & Minerals* **94**, 214–239.

Sitepu, H. (2009) Texture and structural refinement using neutron diffraction data from molybdite (MoO_3) and calcite ($CaCO_3$) powders and a Ni-rich $Ni_{50.7}Ti_{49.30}$ alloy. *Powder Diffraction* **24**, 315–326.

Wooster, N. (1931) The crystal structure of molybdenum trioxide, MoO_3. *Zeitschrift für Kristallographie* **80**, 504–512.

Zhao, J., Ma, P., Wang, J., & Niu, J. (2009) Synthesis and structural characterization of a novel three-dimensional molybdenum–oxygen framework constructed from Mo_3O_9 units. *Chemistry Letters* **38**, 694–695.

Received August 9, 2022. Revised manuscript accepted September 26, 2022.

This manuscript was handled by Associate Editor James Evans and Editor Andrew McDonald.